

# Bistability and long-term cure in a within-host model of hepatitis C

Swati DebRoy<sup>\*†</sup>, Benjamin M. Bolker<sup>‡</sup> and Maia Martcheva<sup>\*</sup>

August 26, 2011

## Abstract

Treatment of hepatitis C virus (HCV) is lengthy, expensive and fraught with side-effects, succeeding in only 50% of treated patients. In clinical settings, short-term treatment response (so-called sustained virological response [SVR]) is used to predict prolonged viral suppression. Although ordinary differential equation (ODE) models for within-host HCV infection have illuminated the mechanisms underlying treatment with interferon (IFN) and ribavirin (RBV), they have difficulty producing SVR without the introduction of an external extinction threshold. Here we show that bistability in an existing ODE model of HCV, which occurs when infected hepatocytes proliferate sufficiently much faster than uninfected hepatocytes, can produce SVR without an external extinction threshold under biologically relevant conditions. The model can produce all clinically observed patient profiles for realistic parameter values; it can also be used to estimate the efficacy and/or duration of treatment that will ensure permanent cure for a particular patient.

KEYWORDS: Hepatitis C, HCV, sustained virological response, SVR, bistability, backward bifurcation.

ABBREVIATIONS: HCV, *Hepatitis C virus*, SVR, *sustained virological response*, DFE, *disease free equilibrium*, EE, *endemic equilibrium*.

## 1 Introduction

Chronic Hepatitis C virus (HCV) infection is a global health problem affecting 3.2 million people in the United States alone. HCV infection, which causes insidious liver damage including chronic hepatitis, cirrhosis and liver cancer [23], is projected to generate medical costs of \$10.7 billion in adults in the US between 2010 and 2019 [30]. Treatment of HCV is sub-optimal, succeeding in only 50% of treated patients and causing several side-effects [15]. Chronic HCV infection can continue for decades, with or without treatment; thus, while treatments for HCV exist, it is hard to know whether they provide an absolute cure for the virus. Rather, the goal of treatment is to achieve *sustained virological response* (SVR), defined as undetectable HCV viral loads six months after the cessation of therapy (Figure 1). SVR is considered a “virological cure” and is usually followed by many years of stable liver function [27].

---

<sup>\*</sup>Department of Mathematics, University of Florida, Gainesville, FL USA

<sup>†</sup>author for correspondence: [swati@ufl.edu](mailto:swati@ufl.edu)

<sup>‡</sup>Departments of Mathematics & Statistics and Biology, McMaster University, Hamilton ON Canada. Second and

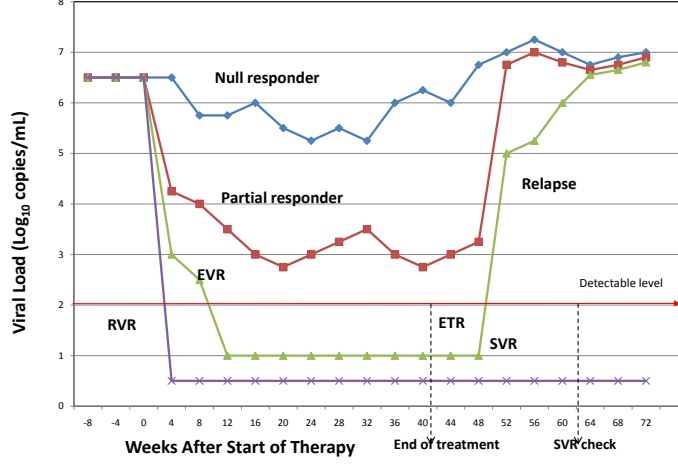


Figure 1: Qualitative viral load (HCV-RNA) dynamics in treated patients, modified from [15]. The detection level is set at 100 copies/mL as stated in [24].

It is becoming increasingly clear that setting universal, fixed treatment durations is impractical. To establish ‘response guided therapy’ [22], clinicians have defined criteria that can be measured during treatment to modify ongoing treatment, as well as to predict the long-term goal of SVR (Figure 1). *End-of-treatment response* (ETR), which is necessary but not always sufficient to achieve SVR, is defined by undetectable viral load at the end of a 24- or 48-week course of therapy. *Rapid virological response* (RVR), which predicts SVR with high probability, is defined as undetectable viral load four weeks into treatment [31, 19]. *Early virological response* (EVR), characterized by  $\geq 2$  log reduction or undetectable viral load at week 12 of therapy, is considered necessary for achievement of SVR [9, 14]. *Relapse* denotes the reappearance of HCV RNA in serum after the end of therapy; *null responders* are patients who fail to achieve a decrease in HCV RNA by 2 logs after 24 weeks of therapy; and *partial non-responders* are those who exhibit 2 log decrease in HCV RNA but are still HCV RNA positive at week 24 [15].

One role of mathematical models is to clarify how variation among patients, and among HCV genotypes, can lead to this array of treatment responses, with the ultimate goal of improving prediction and treatment. Previous immunological models of HCV such as those by Dahari *et al.* [5] and Dixit *et. al.* [11] have made valuable contributions, exploring the factors that determine the efficacy of peg-interferon and ribavirin treatment of HCV. Owing to the short-term nature of available treatment data, initial modeling efforts were geared towards producing short-term responses that accurately mimicked observed data [5, 6]. Although the short-term responses are

---

third authors are alphabetically ordered.

good indicators of future cure, there is an increasing need for models to provide more definite predictions of medium- and long-term viral response. Here, we explore the fact that an existing model of HCV with regeneration (from [5, 26]) has the intrinsic mathematical property of bistability under biologically relevant conditions, so that the system can produce SVR; in fact, we demonstrate that this model can produce all the qualitative treatment profiles shown in Figure 1.

A useful mathematical definition of cure is that after the cessation of treatment the density of the pathogen (defined here as viral load) converges to a stable *disease free equilibrium*, (DFE). That is, while the pathogen is still present at a positive density, that density is continuously decreasing toward zero. In contrast, we characterize chronic infection or failure to cure as convergence toward a stable *endemic equilibrium* (EE) with positive pathogen density. Most current models of within-host dynamics have a single stable equilibrium. In these models, a successful treatment (one to which the patient responds) is characterized by a switch in stability from the EE to the DFE. In this case, pathogen density declines during treatment (sometimes rapidly) toward zero from its pre-treatment equilibrium level. (In other diseases, such as HIV, factors such as the emergence of drug-resistant variants make the switch to a DFE elusive, and the goal switches instead toward lowering the size of the EE to a level which minimizes the effects of disease on the patient.) However, these models typically assume that treatment is lifelong. When treatment stops, these models always predict a rebound, sometimes rapid, back to the pre-treatment EE — that is, they do not predict a cure.

How can we reconcile the observation of effective short-term treatment with the behavior of mathematical models? First, and probably most often cited by mathematical modelers, are the effects of discreteness and stochasticity missing from standard deterministic models. At very low within-host pathogen densities (and numbers), chance events can lead to the pathogen’s complete extinction. Snoeck *et. al.* [29] have recently taken this approach, using an HCV model [6] with regeneration that distinguishes between infectious and non-infectious virions. The threshold criterion they define, based on an expected total of  $< 1$  infected hepatocytes in the patient’s body, allows them to produce all long-term patient responses including SVR.

Second, the post-treatment rebound towards the EE may be so slow that viral levels remain undetectable even beyond the host’s natural lifespan. (This possibility proves to be unlikely for our system, but could be applicable to the within-host dynamics of other pathogens.)

A third possibility, less often explored by modelers (although see [16]), is that the host-pathogen system is *bistable*, meaning that the system could converge to either the DFE or the EE, depending on initial conditions. In this scenario, the patient begins treatment at or near the (stable) EE. While treatment may or may not change the stability of the EE, it can push pathogen densities (and densities of host cells or immune factors) over a threshold, into the so-called *basin of attraction* of the DFE, where the system will naturally approach the DFE in the long run. When treatment ceases, the system remains in basin of attraction of the DFE, the pathogen density continues to decline towards the DFE, and the patient is both clinically and mathematically cured.

A well-established mathematical model of the interaction between treatment, HCV, and host cells is known to allow bistability [26]; however, the implications of this behavior for treatment have not been previously explored in detail. In this paper, we analyze the system of equations to establish mathematical criteria that define when this behavior occurs and show that it does occur for realistic parameter values. In addition, we explore the parameter space numerically to show

that the intrinsic property of bistability allows the model to reproduce all of the patient profiles (null responder, partial responder, SVR, etc.) displayed in Figure 1, without external stimulation. For a particular patient/HCV genotype combination (i.e., a set of model parameters), we can use the model to find the boundaries of the basin of attraction — that is, to define combinations of state variables (viral load and number of uninfected hepatocytes) reached during treatment that will ensure SVR. We use these estimates in turn to predict the minimum treatment time for a particular fixed drug efficacy, or the minimum treatment efficacy for a fixed treatment time.

## 2 Model definition

We use a standard ODE model of the interaction between hepatocytes and HCV [5, 6]:

$$\begin{aligned}\frac{dT}{dt} &= s + r_1 T \left(1 - \frac{T+I}{T_{\max}}\right) - dT - \beta TV \\ \frac{dI}{dt} &= \beta TV + r_2 I \left(1 - \frac{T+I}{T_{\max}}\right) - \delta I \\ \frac{dV}{dt} &= (1 - \epsilon)pI - cV\end{aligned}\tag{1}$$

The three continuous state variables in the model represent the number of uninfected hepatocytes ( $T$ ), infected hepatocytes ( $I$ ) and free virus, or viral load ( $V$ ). Time is measured in days. The model assumes a baseline (absolute) recruitment rate of uninfected hepatocytes at rate  $s$  and a baseline (*per capita*) mortality rate  $d$ . Hepatocytes proliferate in a density-dependent, or homeostatic, way with a maximum proliferation rate  $r_1$  and  $r_2$  for uninfected and infected hepatocytes respectively (as discussed below, this difference is critical for the occurrence of bistability), while the maximum hepatocyte density or ‘carrying capacity’  $T_{\max}$ , is based on both uninfected and infected hepatocytes. Uninfected hepatocytes are infected by free virus at a per-virus, per-hepatocyte rate of  $\beta$ ; thus,  $\beta TV$  is the rate of hepatocyte infection. Infected hepatocytes are cleared, due to natural death, immune response, or drug action, at a *per capita* rate  $\delta$ . Finally, the dynamics of free virus particles in the absence of treatment are determined by  $p$  (rate of production per infected hepatocyte) and  $c$  (clearance rate).

Neumann *et. al.*[24] studied the effect of interferon and ribavirin treatment on HCV patients by fitting a simple dynamical model to data from patients undergoing therapy. This seminal article in modeling the treatment of HCV estimated that treatment had negligible effects on the clearance rates of infected hepatocytes ( $\delta$ ) and free virus ( $c$ ). When the efficacy of treatment on  $p$  was close to 100%, the efficacy of treatment on  $\beta$  was approximately zero. In [5], although the authors incorporate the effect of treatment on both production ( $p$ ) and infection ( $\beta$ ) for mathematical analysis, their numerical solutions combine the efficacies into a single effect acting on  $p$  alone. Here, we analyze the model in absence of treatment and explore the effects of treatment numerically; following [5], we include the effect of treatment on production ( $p$ ) alone, through the efficacy parameter  $\epsilon$ .

This model has been thoroughly analyzed and fitted to available data on patient profiles under treatment [5, 26, 4, 7]. The model appears to be appropriate for understanding the dynamics of *in*

*vivo* HCV infection and possibly hepatitis B (HBV) infection [8]. Dahari *et al* [7] have also studied the relationship among drug efficacy, infected hepatocyte death rate, rate of final phase decline and the baseline fraction of infected hepatocytes before treatment. Another article by Dahari *et al* [4] used the same model to show that a high baseline viral load reduces the chances of achieving SVR. This extensive effort has estimated realistic ranges for all of the parameters which we use hereafter.

The *basic reproduction number* ( $\mathcal{R}_0$ ) is a standard metric in epidemiology and in within-host dynamics that describes the ability of a pathogen to spread after its initial introduction. In this case,  $\mathcal{R}_0$  can be interpreted as the total number of secondary hepatocyte infections caused by a single infected hepatocyte when it is introduced into a completely susceptible population of hepatocytes.

The  $\mathcal{R}_0$  of (1) without treatment is given by

$$\mathcal{R}_0 = \frac{\beta p}{c\delta} T_0 + \frac{r_2}{\delta} \left( 1 - \frac{T_0}{T_{\max}} \right), \quad (2)$$

where  $T_0$  is the concentration of uninfected hepatocytes at the DFE,  $(T_0, 0, 0)$ , given by

$$T_0 = \frac{T_{\max}}{2r_1} \left( (r_1 - d) + \sqrt{(r_1 - d)^2 + 4s \frac{r_1}{T_{\max}}} \right)$$

[5]. The first term in (2) accounts for the fact that the infected hepatocyte can produce up to  $p$  virions in its lifetime of  $\frac{1}{c}$  days and each virus can infect a uninfected hepatocyte at the rate  $\beta$  over its lifetime of  $\frac{1}{\delta}$  days. The second term accounts for the number of infected hepatocytes produced by proliferation from the introduced infected hepatocyte.

### 3 Bistability: mathematical analysis

A *bifurcation* is a set of parameter values where equilibria appear, disappear or change stability. The *bifurcation curve* maps this change with respect to a *bifurcation parameter* [2]: for example, the bifurcation curve shown in Figure 2 depicts changes in the value and stability of equilibria as a result of changes in the clearance parameter  $\delta$ , holding all other parameters fixed (equivalent to changing  $\mathcal{R}_0$ ). The DFE is locally stable for  $\mathcal{R}_0 < 1$  and unstable for  $\mathcal{R}_0 > 1$ . Thus  $\mathcal{R}_0 = 1$  is a bifurcation point.

If a stable EE exists for some range of  $\mathcal{R}_0 < 1$  as well as in the region with  $\mathcal{R}_0 > 1$ , the model is said to exhibit *backward bifurcation* [20]. In this case both the DFE and the EE can be stable in a region with  $\mathcal{R}_0 < 1$  (*bistability*). Which equilibrium the system approaches depends on the starting values of the state variables ( $T$ ,  $I$ , and  $V$ ). Figure 2 shows the bifurcation curve for model 1, without treatment, with biologically relevant values of parameters, showing the equilibrium quantities per mL of free virus ( $V^*$ ) as a function of  $\mathcal{R}_0$  as the bifurcation parameter  $\delta$  varies. We use  $\mathcal{R}_c$  to denote the left-most point on the bifurcation curve where the EE exists (i.e. lowest  $\mathcal{R}_0$ , and the highest  $\delta$ ; low values of  $\mathcal{R}_0$  correspond to high values of  $\delta$ ).

When a backward bifurcation occurs, there are at least three equilibria in the region  $\mathcal{R}_c < \mathcal{R}_0 < 1$ : the stable DFE, a large stable EE and a smaller unstable EE which separates the basins of attraction of the two stable equilibria [20]. In this model we observe that a backward bifurcation

can occur only if  $r_2 > r_1$ , i.e., if the rate of proliferation of infected hepatocytes is greater than the proliferation rate of uninfected hepatocytes. Although one might expect that infected hepatocytes would always proliferate slower rather than faster than uninfected ones because their function would be impaired by viral infection, studies of tissues from hepatocellular carcinoma patients show that HCV can enhance infected hepatocyte turnover in order to replace cells destroyed by immunological attack [1].

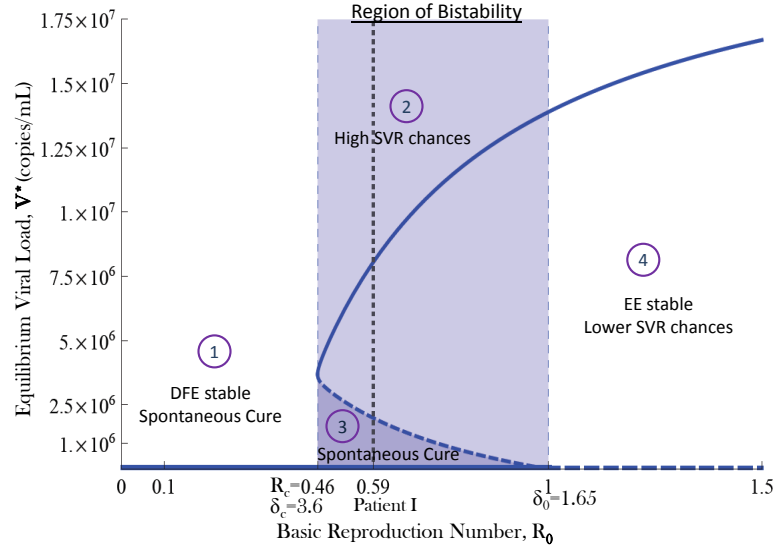


Figure 2: A bifurcation curve for the model with bifurcation parameter  $\delta$ . Clearance rate  $\delta$  ranges from  $16.56$ – $1.1$  while  $R_0$  ranges from  $0.1$ – $1.5$  (the realistic range for  $\delta$  is between  $1.4 \times 10^{-3}$  and  $3.0 \text{ day}^{-1}$  [7]). Other parameters:  $s = 3661.7$ ,  $T_{\max} = 6.33 \times 10^6$ ,  $d = 1.4 \times 10^{-3}$ ,  $\beta = 7.4 \times 10^{-8}$ ,  $p = 40.5$ ,  $c = 11.5$ ,  $r_1 = 0.31$ ,  $r_2 = 4.4$ . Unrealistic (i.e. negative) equilibria are not shown.

A particular choice of model parameters describes the characteristics of a particular patient phenotype infected with a particular viral genotype: we refer interchangeably to “parameter sets” and simulated (*in silico*) “HCV patients”. Each patient/set of parameters corresponds to a particular  $R_0$  in Figure 2. Depending on a patient’s  $R_0$  and the corresponding EE (represented in the Figure by viral load), a patient can fall in any of the four distinct regions shown in the Figure 2.

- Patients with low  $R_0$  (Figure 2, region 1) should spontaneously clear the virus, because the DFE is stable and the EE does not exist. These patients would probably never require medical intervention.
- When  $R_0 \geq 1$  (region 4) the natural dynamical properties of the model will not predict SVR (in [29] this is achieved by reducing the density of infected hepatocytes to zero when it goes below a critical quantity corresponding to a single hepatocyte per patient). Here the DFE exists but is unstable, while the EE is stable. Patients in this region will always rebound to their original viral load once treatment stops — they will never achieve SVR.

- In the central (shaded) region, the model is bistable. Three equilibria viz., a stable DFE, a stable EE, and an unstable equilibrium between them, exist. Patients whose pre-treatment state (viral load) falls in region 3 will behave like those in region 1, exhibiting spontaneous cure. Those who fall within region 2 will establish a stable EE in the absence of treatment, similar to those in region 4. Unlike patients in region 4, however, treatment may push the viral load down into region 3, leading to SVR. Regions 2 and 3 are separated by the unstable endemic equilibrium which represents as a viral load threshold for permanent cure.

We first analytically define the conditions that determines if a parameter set lies in the bistable region (2 and 3).

Bistability occurs under the following conditions (derived in Appendix A):

$$\mathcal{R}_0 < 1 \tag{3}$$

$$r_2 - r_1 > \frac{s}{T_0^2} \frac{r_2}{\tilde{\beta}} + \tilde{\beta} T_{\max}, \tag{4}$$

where  $\tilde{\beta} = \beta_c^p$ . The second condition implies that  $r_2 > r_1$ ; the proliferation rate of infected hepatocytes must be greater than that of uninfected hepatocytes. When  $r_2$  is sufficiently greater than  $r_1$ , even when  $\mathcal{R}_0 < 1$ , the system can keep producing enough new infected hepatocytes and in turn enough free virus that a non-zero EE can be stable.

The bistability criteria also allows us to determine the region of bistability defined by the range of values of the bifurcation parameter for which bistability occurs. The criterion  $\mathcal{R}_0 = 1$  allows us to determine  $\delta_0$ , which defines the upper boundary of the bistable region. Following the calculation process in [16], we can then determine the critical value of  $\delta_c$  corresponding to  $\mathcal{R}_c$ , the lower boundary of the bistable region (Appendix A).

## 4 Numerical exploration of parameter space: patient profiles

### 4.1 Observed Patient Profiles

With the properties of bistability behavior in model 1 we first show that it is possible to simulate all the four distinct types of patient profiles shown in Figure 2 (Figure 3). We took parameters from the literature [5, 6] to represent patient profiles where short-term treatment responses, but not SVR, are possible ( $\mathcal{R}_0 > 1$ ) to produce naturally. To find realistic parameter sets which satisfy the criteria for backward bifurcation ( $\mathcal{R}_c < \mathcal{R}_0 < 1$ : 4), and hence SVR can be simulated in the model, we randomly drew parameters from uniform distributions with the criterion  $r_2 > r_1$ , and within the ranges given in Dahari et al [4, 7] (details in Appendix B).

As noted before, a mathematical representation of cure, such that the viral load decreases continuously to zero even after the cessation of treatment, is impossible for  $\mathcal{R}_0 > 1$ . Even if the patient is treated with a highly effective regimen for a long time, relapse occurs almost instantaneously after therapy cessation. For patients in this category we can generate profiles for null and partial responders, EVR, and RVR. However SVR (see Figure 3(a)) cannot be produced without imposing

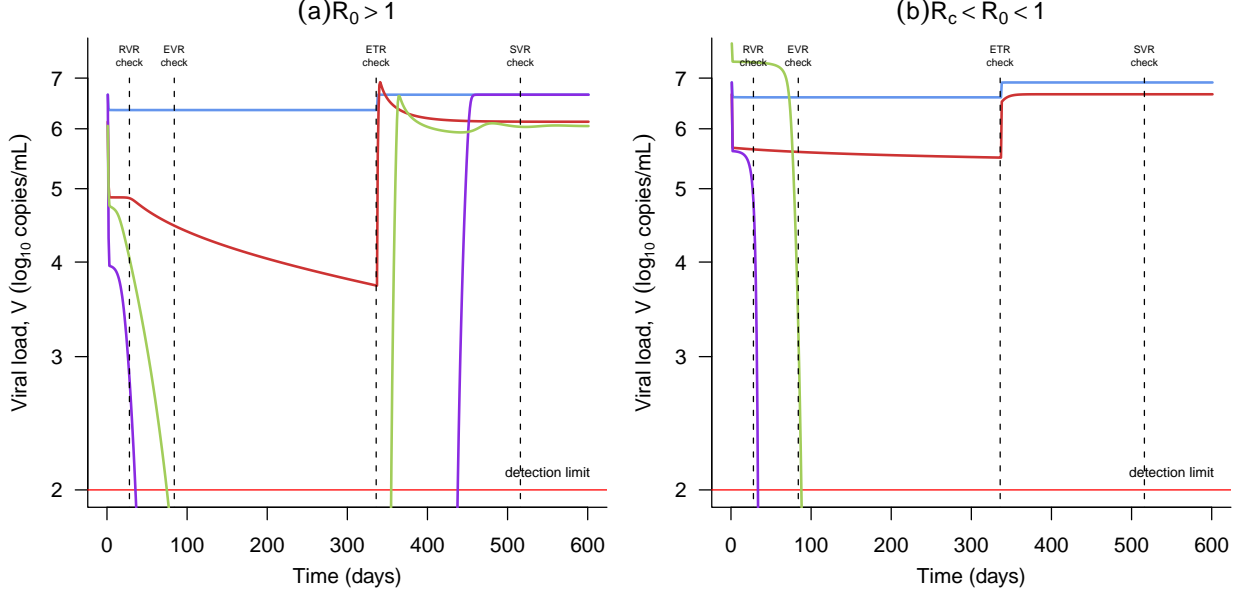


Figure 3: Patient profiles. In all cases, patients start from the stable EE in the absence of treatment. Treatment begins at time  $t = 0$  and lasts for the standard period of 48 weeks = 336 days. (a) Patients where only short-term treatment response is possible ( $\mathcal{R}_0 > 1$ ), without the achievement of SVR. **Null responder:**  $s = 2.6 \times 10^4$ ,  $T_{\max} = 1 \times 10^7$ ,  $d = 2.6 \times 10^{-3}$ ,  $\beta = 2.25 \times 10^{-7}$ ,  $p = 2.9$ ,  $c = 6.0$ ,  $r_1 = 4.2$ ,  $r_2 = 4.2$ ,  $\delta = 0.26$  [5] and  $\epsilon = 0.5$ . **Partial responder:**  $s = 4$ ,  $T_{\max} = 9.13 \times 10^6$ ,  $d = 1.3 \times 10^{-2}$ ,  $\beta = 3.5 \times 10^{-7}$ ,  $p = 4.3$ ,  $c = 3.5$ ,  $r_1 = 0.5$ ,  $r_2 = 0.25$ ,  $\delta = 0.22$  [6] and  $\epsilon = 0.945$ . **RVR** (with relapse): as null responder, but with higher treatment efficacy ( $\epsilon = 0.998$ ). **EVR** (with relapse):  $s = 7.3$ ,  $T_{\max} = 0.51 \times 10^7$ ,  $d = 12.9 \times 10^{-3}$ ,  $\beta = 3.5 \times 10^{-7}$ ,  $p = 4.4$ ,  $c = 3.5$ ,  $r_1 = 0.5$ ,  $r_2 = 0.25$ ,  $\delta = 0.22$  [6], and  $\epsilon = 0.94$ . (b) Patients where SVR is possible to produce dynamically ( $\mathcal{R}_c < \mathcal{R}_0 < 1$ ). **Null responder:**  $s = 3661.7$ ,  $T_{\max} = 6.33 \times 10^6$ ,  $d = 1.4 \times 10^{-3}$ ,  $\beta = 7.4 \times 10^{-8}$ ,  $p = 40.5$ ,  $c = 11.5$ ,  $r_1 = 0.31$ ,  $r_2 = 4.4$ ,  $\delta = 2.8$  and  $\epsilon = 0.5$ . **Partial responder:**  $s = 4.1 \times 10^3$ ,  $T_{\max} = 1.2 \times 10^7$ ,  $d = 1.3 \times 10^{-3}$ ,  $\beta = 7 \times 10^{-7}$ ,  $p = 5.8$ ,  $c = 19.46$ ,  $r_1 = 2.1 \times 10^{-1}$ ,  $r_2 = 5.1$ ,  $\delta = 2.5$  and  $\epsilon = 0.9$ . **RVR:** as null responder, but with higher treatment efficacy ( $\epsilon = 0.95$ ). **EVR:**  $s = 5133$ ,  $T_{\max} = 9.9 \times 10^6$ ,  $d = 1.3 \times 10^{-3}$ ,  $\beta = 1.57 \times 10^{-08}$ ,  $p = 43$ ,  $c = 5.09$ ,  $r_1 = 1.4$ ,  $r_2 = 4.8$ ,  $\delta = 1.35$  and  $\epsilon = 0.62$ .

further external criteria. Furthermore, even the patients who are able to show RVR do not achieve SVR in our model simulations, although RVR is a very good indicator of SVR in reality. Thus model 1 never predicts cure for patients with such parameter combinations when allowed to run normally.

We have not ruled out the possibility that there exist parameters where treatment for the standard duration could lead to realistic short-term dynamics and a long-term rebound that is so slow that, despite the eventual theoretical return to the EE, the viral load does not increase above the detection level (100 copies/ml) during the expected lifetime of the patient  $t \gg 600$  days. Similarly, there may be parameter combinations for the bistability case (Figure 3(b)) that display relapse: i.e. the viral load drops below detection level during treatment, but not into the basin of attraction of the DFE, so that the viral load returns to pre-treatment levels once treatment is



stopped. However, we were unable to find parameter sets that satisfied either of these profiles (SVR for  $\mathcal{R}_0 > 1$  or relapse for  $\mathcal{R}_c < \mathcal{R}_0 < 1$ ) for realistic parameter values.

## 4.2 Estimating critical treatment efficacy and duration

In this section, we explore the effects of different treatment strategies for a fixed parameter set in the bistability regime. Here we provide a "proof of concept" example of what can be achieved using this model for a specific class of patients whose parameters might exhibit bistability. We define a "Patient I" according to the parameter set shown in Figure 2 with  $\delta$  fixed at  $2.8 \text{ day}^{-1}$ . We assume that a chronic patient who requires treatment (will not clear the virus spontaneously) has the state variables at the stable EE. In that case we study the regions of attraction of the EE and DFE, and what combinations of treatment efficacy and duration will be sufficient to drive a patient from the EE into the basin of attraction of the DFE where permanent cure will occur.

For illustrative purposes, we reduce the three-dimensional  $\{T, I, V\}$  system to a planar ( $\{T, V\}$ ) system with very similar dynamical properties. Because free virus  $V$  has very rapid dynamics relative to those of  $T$  and  $I$ , free virus will quickly equilibrate to a quasi-equilibrium level, and thus if we know  $V$  we can estimate the current density of infected hepatocytes. Substituting this value  $\hat{I} = \frac{c}{p}V$ , the model 1 reduces to:

$$\begin{aligned}\frac{dT}{dt} &= s + r_1 T \left(1 - \frac{T + \frac{c}{p}V}{T_{\max}}\right) - dT - \beta TV \\ \frac{dV}{dt} &= \tilde{\beta}TV + r_2 V \left(1 - \frac{T + \frac{c}{p}V}{T_{\max}}\right) - \delta V.\end{aligned}\tag{5}$$

The reduced model (5) has the same equilibria and similar bifurcation properties as the original model (1). We first plot the dynamics for Patient I in the phase plane with  $V$  (viral load) and  $T$  (uninfected hepatocytes) on the axes, to visualize the basins of attraction of the DFE and the EE (Figure 4). The figure is an expanded representation of the marked point in Figure 2 that indicates the parameters corresponding to Patient I ( $\delta = 2.8$ ,  $\mathcal{R}_0 = 0.59$ ), showing the full phase plane rather than just the equilibrium values of viral load; the qualitative picture is the same throughout the bistability regime. The figure shows the trajectory of Patient I, starting from the EE before treatment, during and after treatment. The viral load initially falls very rapidly, then more slowly as the patient's uninfected hepatocyte population recovers toward the DFE. When treatment stops, there is an immediate, rapid, but also temporary rebound of the viral load. After a brief increase, the viral load again begins to decrease toward zero as the hepatocyte population continues to recover toward the DFE. Thus, the patient can maintain SVR without further treatment.

The continued recovery of the patient is entirely due to the fact that treatment was continued long enough to drive the patient's state from the stable EE across the boundary into the basin of attraction of the DFE. If treatment were less effective or applied for a shorter period, the viral load would instead have increased (and the uninfected hepatocyte population decreased) back to the stable EE after the end of treatment.

Figure 4 shows that one must increase the population of uninfected hepatocytes as well as lower the viral load in order to attain SVR (i.e., move to the right [increasing  $T$ ] as well as down

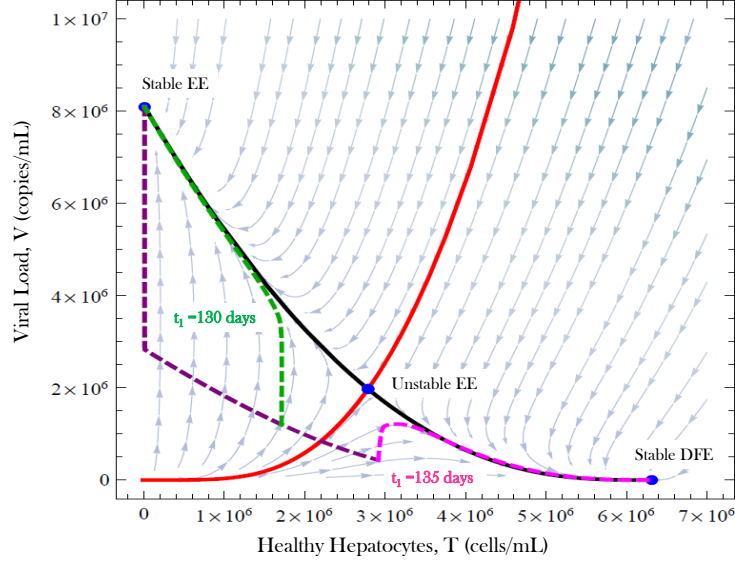


Figure 4: Phase plot for Patient I based on the reduced model (5). The purple line shows the trajectory through  $\{T, V\}$  space of Patient I during treatment (with  $\epsilon = 0.65$ ), starting at the stable EE (upper left corner), simulated using the original model (1). When treatment stops after 130 days, the viral load follows the green dashed line and returns to the stable EE and the patient is not cured. Whereas, if the treatment is allowed to continue for 135 days, the trajectory continues along the (magenta line) to converge to the (stable) DFE. Blue points represent equilibria; the red line (the *separatrix*) shows the threshold in phase space dividing states from which the patient will relapse (upper left side) or recover (lower right side); the black line shows the stable manifold, along which the system will tend to travel in the absence of treatment.

[decreasing  $V$ ] in order to cross the threshold). This phenomenon can explain the fact that cirrhotic patients of lower viral load are harder to treat, than non-cirrhotic patients with higher viral loads, as observed by Dahari *et al* [4]. Since the concentration of uninfected hepatocytes is considerably lower in a cirrhotic patient (and their recruitment and proliferation rates may be impaired as well), treating to reach the basin of attraction of the DFE where SVR will occur is harder.

In the bistable regime, the model allows us to numerically explore the effectiveness and duration of treatment necessary to push the state variables into the the basin of attraction of the DFE, so that the patient will spontaneously clear the virus. We shall modulate the effects of treatment by changing the efficacy ( $\epsilon$ ) and the duration of treatment ( $t_1$ ).

Figure 5(a) shows the same basic dynamics as Figure 4, but with differing levels of efficacy so that the treatment time of  $t_1 = 48$  weeks may or may not be sufficient to drive the patient into the basin of attraction of the DFE and induce SVR. For low  $\epsilon$ , the patient returns to pre-treatment viral load after cessation of therapy, while for high  $\epsilon$  (and the same treatment period) they achieve SVR.

We can use the same general approach to adjust the time of treatment, rather than the efficacy. While one would always like to treat with as close to 100% efficacy as possible, in fact different patients experience different efficacies (typically due to weak immune responses). In this case, one

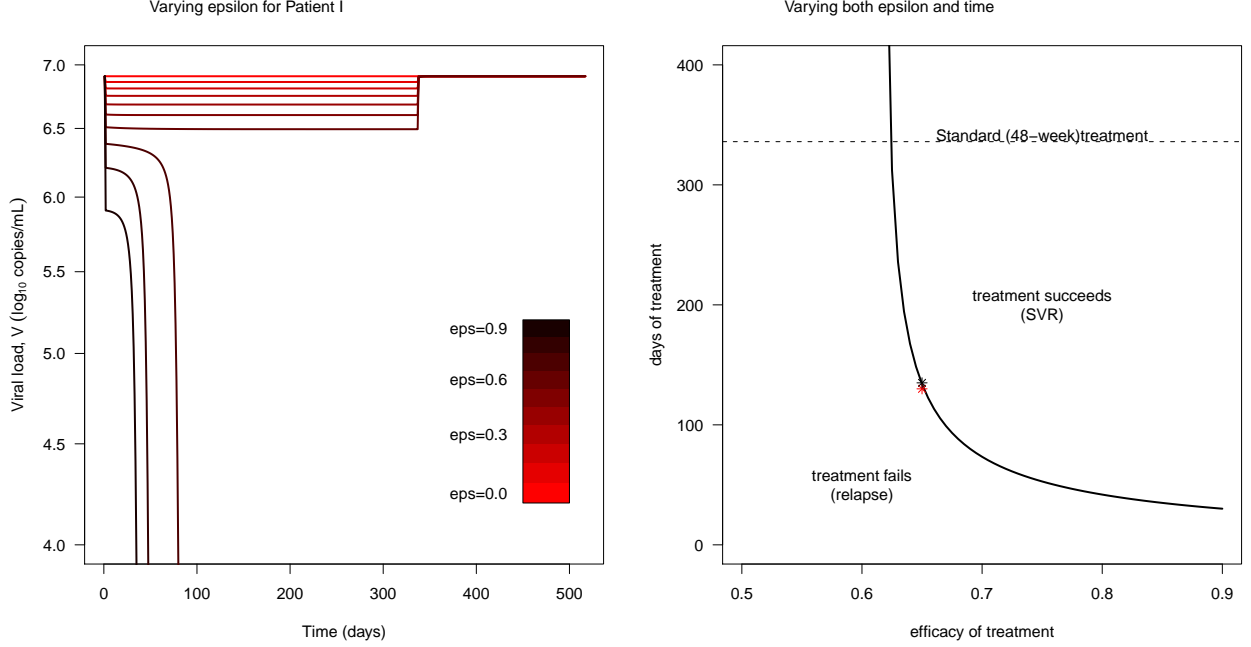


Figure 5: (a): viral response as efficacy of drug,  $\epsilon$  is increased from 0 to .9, by .1 when treated for a fixed period of time,  $t_1 = 48$  weeks, and checked for SVR 6 months later. (b): The optimal period of treatment necessary to achieve SVR for a range of  $\epsilon$ s lies on the black curve. The  $\epsilon$  and  $t_1$  combinations to the right of this curve will result in SVR, and the ones on the left will cause relapse. The stars represent the combination used to produce the 2 treatment trajectories in figure 4.

can increase the duration of treatment to facilitate SVR. Jensen *et. al.* [18] found that increasing the treatment duration to 72 weeks when re-treating previous non-responders yielded more SVR.

Figure 5(b) shows the relationship between critical efficacy  $\epsilon$  and treatment time  $t_1$  to achieve SVR for the same parameters (Patient I) explored previously. Below an efficacy of  $\approx 0.62$ , the required treatment time increases rapidly beyond the treatment time of 48 weeks (336 days). Since the general intention of the doctors is to reduce the treatment duration, most patients do not get treated for more than 48 weeks. With an efficacy of  $\approx 0.74$ , the treatment time can be reduced to 50 days, but further increases in treatment efficacy do not further decrease the required treatment time.

## 5 Discussion

Mathematical models of HCV dynamics *in vivo* [21, 24, 5] have improved our understanding of several aspects of this disease.

Due to the nature of the available data, most existing models of HCV dynamics *in vivo* have

focused on the short term effects of treatment. While standard ODE models do a reasonably good job predicting long-term results like SVR (itself a proxy for indefinite suppression of virus and maintenance of liver function), they are unable to produce SVR from direct model simulations. Thus, a disconnect remains between the long-term behavior of models and real patients. Snoeck *et al.* [29] bridge this gap by imposing an external extinction threshold; here, in contrast, we have explored the implications of bistability in a simple ODE for long-term cure of treated patients.

Most previous analyses of bistability have focused at the population, or epidemiological, level [20, 12, 13]. In one of the few previous studies to explore bistability in an immunological (*in vivo*) model, Gomez-Acevedo and Li [16] used backward bifurcation to explain the viral dynamics of HTLV-I infection and encourage treatment measures to consider the more difficult threshold that needs to be overcome to achieve cure in case of bistability. Qesmi *et al.* [25] have also interpreted bistability as posing a higher threshold for successful treatment, when HCV and HBV (hepatitis B virus) infection is considered in both blood and liver. In most models of disease control, at either the within-host or within-population level, controls are introduced (e.g. vaccination given to TB patients: [20]) to permanently change a population parameter such that  $\mathcal{R}_0 < \mathcal{R}_c$ . The disease is then driven to DFE. In the case of HCV, the effect of treatment is only temporary and thus the viral system of a single patient cannot move horizontally in Figure 2; we can only permanently change the state variables, not the system parameters. Thus, in contrast to previous studies, we interpret bistability as a benefit — only in the bistable case can we use a temporary period of treatment to achieve permanent control of a disease *in vivo*.

The bistability property of model 1 allows us to simulate all the distinct patient profiles that are observed under treatment (Figure 1). For disease parameters that do not imply spontaneous viral clearance (i.e.  $\mathcal{R}_0 > \mathcal{R}_c$ ), we can reproduce the qualitative outcomes of null responders, partial responders, EVR, and RVR whether one or two stable equilibria exist. However, SVR occurred only under bistability ( $\mathcal{R}_c < \mathcal{R}_0 < 1$ ) and relapse occurred only with a single stable equilibrium ( $\mathcal{R}_0 > 1$ ).

We cannot rule out the possibilities of producing long term viral suppression for  $\mathcal{R}_0 > 1$  by stochastic extinction [29] or slow rebound (the former seems unlikely on the basis of our numerical exploration, although [29] *et al.* did see realistic rebound patterns in their model). Further investigation will be necessary to differentiate these hypotheses. Our aim in this article is to introduce bistability as a plausible alternative hypothesis to understand HCV treatment dynamics.

In order for bistability to occur in this model, the rate of proliferation of infected hepatocytes must be greater than that of the uninfected hepatocytes; *in vivo* studies [1] have shown that this counterintuitive condition is biologically plausible. Given the disease parameters of a patient we can (1) establish whether bistability occurs and (2) establish bounds on efficacy and duration of treatment. Thus, we can determine the treatment thresholds for sustained clearance of the virus, or predict the qualitative response for any particular combination of efficacy and duration of treatment. These kinds of numerical investigations (ideally with better bounds on the parameter values and more realistic models) could be especially valuable in the context of recent suggestions to adjust the duration of treatment on the basis of patient responses [22]. Our approach, which finds the shortest treatment or lowest drug efficacy that will lead to long-term cure, is complementary to other modeling efforts that have focused on minimizing side-effects by optimally controlling the

reduction of viral load [3] or by treating with epoetin to increase red blood cell count [10].

Our very simple mathematical representation of viral infection in the human liver neglects many of the complexities of human physiology and the immunobiology of the hepatitis C virus. Furthermore, since parameters must be estimated from short-term patient data, the uncertainty on parameter ranges are very wide [7, 4]. To make useful predictions for individual patients, disease parameters will need to be estimated from even shorter periods of treatment response, perhaps with the assistance of information based on clinical biomarkers. Use of within-host models as diagnostic and management tools is well known by now [17], but still presents many practical challenges even in established areas like HIV treatment [28].

However, we have demonstrated a new way to think about the long term dynamics of HCV infection within hosts. In principle this model could ultimately develop into a clinical predictive or management tool.

## 6 Acknowledgements

The authors would like to thank Dr. Fabio Milner for suggesting this approach for the problem. SDR and MM are partially supported by NSF grant DMS-0817789 and BMB is partially supported by NIH ROI grant GM083192. SDR thanks Dr. Carlos Castillo-Chavez for his critical guidance during MTBI-2009 (supported by NSF DMP-0838704, NSA H98230-09-1-0104, the Alfred P. Sloan Foundation, and the Office of the Provost of Arizona State University) where the fundamentals of this article were prepared. SDR appreciates the help and support of Dr. Anuj Mubayi, Dr. Christopher Kribs-Zaleta and Dr. Marco Herrera during MTBI-2009. We also thank the anonymous reviewers who have helped us improve the manuscript.

## A Appendix: Analysis

We first explore the conditions under which the model, without treatment, will have multiple equilibria. We define  $(T^*, I^*, V^*)$  as an equilibrium point, satisfying

$$0 = s + r_1 T^* \left(1 - \frac{T^* + I^*}{T_{\max}}\right) - dT^* - \beta T^* V^* \quad (6)$$

$$0 = \beta T^* V^* + r_2 I^* \left(1 - \frac{T^* + I^*}{T_{\max}}\right) - \delta I^* \quad (7)$$

$$0 = pI^* - cV^* \quad (8)$$

Equation 8 leads to  $V^* = \frac{p}{c}I^*$ , which allows us to reduce (6–8) to two equations. Defining  $T^* = f(I^*)$ , we (6) as

$$s + r_1 f(I^*) \left(1 - \frac{f(I^*) + I^*}{T_{\max}}\right) - df(I^*) - \tilde{\beta} f(I^*) I^* \quad (9)$$

where  $\tilde{\beta} = \beta \frac{p}{c}$ . To compute the *disease-free equilibrium* (DFE) we assume  $I^* = V^* = 0$ , giving the concentration of uninfected hepatocytes without infection  $T_0 := f(0) = \frac{T_{\max}}{2r_1} \left( (r_1 - d) + \sqrt{(r_1 - d)^2 + 4s \frac{r_1}{T_{\max}}} \right)$ .

If we specify that the equilibrium considered is an *endemic* equilibrium, then  $I^* > 0$ . We simplify and redefine (7) as a function  $F(I^*)$ :

$$F(I^*) = \frac{\tilde{\beta}}{\delta} f(I^*) + \frac{r_2}{\delta} \left( 1 - \frac{f(I^*) + I^*}{T_{\max}} \right). \quad (10)$$

Note that  $f(0) = T_0$ , and

$$\begin{aligned} F(0) &= \frac{\tilde{\beta}}{\delta} T_0 + \frac{r_2}{\delta} \left( 1 - \frac{T_0}{T_{\max}} \right) \\ &= \mathcal{R}_0 \\ \mathcal{R}_0 &= \frac{D}{\delta}, \end{aligned}$$

where  $D = \frac{1}{\delta} \left( \tilde{\beta} T_0 + r_2 \left( 1 - \frac{T_0}{T_{\max}} \right) \right)$

The non-negative real roots of  $F(I^*) = 1$  give the concentration of infected hepatocytes at endemic equilibria. Geometrically, we can interpret this as the number of times the parabola  $F(I^*)$  intersects  $F(I^*) = 1$  in the first quadrant of the  $F - I^*$  plane. Clearly, if  $\mathcal{R}_0 = F(0) > 1$ , there is only one endemic equilibrium. If  $\mathcal{R}_0 = F(0) < 1$ , then the parabola can intersect the line, zero, once or twice, leading to the corresponding number of endemic equilibria. To ensure at least one intersection/equilibrium, the slope of the curve at  $I^* = 0$  should be positive. Thus we proceed to calculate  $F'(I^*)$ .

$$F'(I^*) = \left( \tilde{\beta} - \frac{r_2}{T_{\max}} \right) \frac{f'(I^*)}{\delta} - \frac{r_2}{\delta T_{\max}}. \quad (11)$$

$F'(I^*)$  depends on  $f'(I^*)$ , so we calculate

$$f'(I^*) = - \left( \frac{r_1}{T_{\max}} + \tilde{\beta} \right) \left( \frac{r_1}{T_{\max} + \frac{s}{f(I^*)^2}} \right)^{-1}. \quad (12)$$

Since  $f'(I^*)$  is always  $< 0$ , the sign of  $F'(I^*)$  depends on  $(\tilde{\beta} - r_2)$ . Hence:

**Observation 1.** *For  $\mathcal{R}_0 > 1$ , a unique endemic equilibrium exists. For  $\mathcal{R}_0 < 1$ , either*

1. *when  $(\tilde{\beta} - \frac{r_2}{T_{\max}}) > 0$ , there is no non-negative Endemic Equilibrium.*
2. *when  $(\tilde{\beta} - \frac{r_2}{T_{\max}}) < 0$ , at most 2 non-negative Endemic Equilibria may exist.*

Since we are primarily interested in the case when 2 endemic equilibria are present, we impose the *necessary* condition,  $(\tilde{\beta} - \frac{r_2}{T_{\max}}) < 0$ , on our parameters henceforth. We take  $\delta$  as the bifurcation parameter, and define  $F(I^*)$  as a function of  $\mathcal{R}_0$  from equation  $F(I^*) = 1$  as

$$F(I^*) = \frac{\mathcal{R}_0}{D} \left[ \tilde{\beta} f(I^*) + r_2 \left( 1 - \frac{f(I^*) + I^*}{T_{\max}} \right) \right].$$

For a backward bifurcation to occur we require the gradient  $\frac{\partial \mathcal{R}_0}{\partial I^*}|_{\{I^*=0\}} < 0$ . From (10) we get

$$\begin{aligned}\frac{\partial F(I^*)}{\partial I^*} &= \frac{\partial F(I^*)}{\partial I^*} + \frac{\partial F(I^*)}{\partial \mathcal{R}_0} \frac{\partial \mathcal{R}_0}{\partial I^*} \\ &= 0 \\ \frac{\partial \mathcal{R}_0}{\partial I^*}|_{\{I^*=0\}} &= \mathcal{R}_0 \frac{\frac{r_2}{T_{\max}} - \left(\tilde{\beta} - \frac{r_2}{T_{\max}}\right) f'(0)}{\tilde{\beta} T_0 + r_2 \left(1 - \frac{T_0}{T_{\max}}\right)}\end{aligned}\quad (13)$$

On the right hand side of (13), both  $\mathcal{R}_0$  and the denominator are always positive. Hence for the expression to be negative we require  $\frac{r_2}{T_{\max}} - \left(\tilde{\beta} - \frac{r_2}{T_{\max}}\right) f'(0) < 0$ . That is,

$$\frac{r_2}{T_{\max}} \left( \frac{s}{T_0^2} + \frac{r_1}{T_{\max}} \right) + \left( \tilde{\beta} - \frac{r_2}{T_{\max}} \right) \left( \tilde{\beta} + \frac{r_1}{T_{\max}} \right) < 0. \quad (14)$$

This inequality can be re-written as

$$r_2 - r_1 > \frac{s}{T_0^2} \frac{r_2}{\tilde{\beta}} + \tilde{\beta} T_{\max} \quad (15)$$

Note that, the right hand side of the above inequality is a positive quantity. Hence we conclude that  $r_2$  has to be sufficiently larger than  $r_1$  for bistability to occur.

## B Appendix: Parameter Selection

To ensure that the bistability condition could be satisfied with a realistic parameter set, we used parameter ranges from the literature as tabulated in Table 1. We first drew the parameters  $T_{\max}, d, s, r_1, \beta, p$  and  $c$  from an uniform distribution. We then drew  $r_2$  such that the second of the conditions (4) were satisfied. Based on these parameters, we then calculate a range for the bifurcation parameter  $\delta$ :  $\mathcal{R}_0 = 1$  gives us  $\delta_0$ , and the calculation of [16] gives us the value of  $\delta_c$ . All values such that  $\delta_0 < \delta < \delta_c$  generate bistability. We drew  $\delta$  from an uniform distribution in the intersection between  $(\delta_0, \delta_c)$  and  $(d, 3)$  as given in Table 1.

Once we have defined a parameter set, we determine whether the corresponding patient would spontaneously be cured, or the range of efficacy  $\epsilon$  that can generate SVR over a range of treatment duration  $t_1$ , and create figures analogous to 5(a & b) and 4 for inspection. We selected a parameter set that produced good illustrations as Patient I. Extreme cases where very high efficacy was required for a long time, to achieve SVR were also observed.

## References

- [1] T. M. Block, A. S. Mehta, C. J. Fimmel, and R. Jordan. Molecular viral oncology of hepatocellular carcinoma. *Oncogene*, 22:5093–5107, 2003.

parameter	interpretation	minimum	maximum	Source
$T_{\max}$	maximum hepatocyte concentration in a liver	$0.4 \times 10^7$	$1.3 \times 10^7$	[7]
$d$	natural death rate of $T$	$1 \times 10^{-3}$	$1.4 \times 10^{-3}$	[7]
$s$	natural production rate of $T$	1	$d \times T_{\max}$	[4, 7]
$r_1$	maximum proliferation rate of $T$	0.1	3	[7]
$\beta$	rate of new infections	$1 \times 10^{-8}$	$1 \times 10^{-6}$	[7]
$\delta$	clearance rate of $I$	$d$	3	[7]
$r_2$	maximum proliferation rate of $I$	1	10	[4] (for $r_1$ )
$p$	proliferation rate of $V$	0.1	45	[4]
$c$	clearance rate of $V$	0.8	22	[7]

Table 1: Realistic range for model parameters

- [2] F. Brauer and C. Castillo-Chavez. *Mathematical Models in Population Biology and Epidemiology*. Springer-Verlag, New York.
- [3] S. P. Chakrabarty and H. R. Joshi. Optimally controlled treatment strategy using interferon and ribavirin for hepatitis C. *Journal of Biological Systems*, 17(1):97–110, 2009.
- [4] H. Dahari, J. E. Layden-Almer, E. Kallwitz, R. M. Ribieiro, S. J. Cotler, T. J. Thomas, and A. S. Perelson. A mathematical model of hepatitis C virus dynamics in patients with high baseline viral loads or advanced liver disease. *Gastroenterology*, 136:1402 – 1409, 2009.
- [5] H. Dahari, A. Loa, R. M. Ribeiroa, and A. S. Perelson. Modeling hepatitis C virus dynamics: Liver regeneration and critical drug efficacy. *Journal of Theoretical Biology*, 247:371–381, 2007.
- [6] H. Dahari, R. M. Ribeiro, and A. S. Perelson. Triphasic decline of hepatitis C virus RNA during antiviral decline. *Hepatology*, 46:16–21, July 2007.
- [7] H. Dahari, E. Shudo, S. J. Cotler, T. J. Layden, and A. S. Perelson. Modelling hepatitis C virus kinetics: the relationship between the infected cell loss rate and the final slope of viral decay. *Antiviral Therapy*, 14:459–464, 2009.
- [8] H. Dahari, E. Shudo, R. M. Ribieiro, and A. S. Perelson. Modeling complex decay profiles of hepatitis B virus during antiviral therapy. *Hepatology*, 49(32-38), 2009.
- [9] G. L. Davis, J. B. Wong, J. G. McHutchison, M. P. Manns, J. Harvey, and J. Albrecht. Early virologic response to treatment with peginterferon alfa-2b plus ribavirin in patients with chronic hepatitis C. *Hepatology*, 38(3):645–652, Sept 2003.
- [10] S. DebRoy, C. Kribs-Zaleta, A. Mubayi, G. Cardona-Melendez, L. Medina-Rios, M. Kang, and E. Diaz. Evaluating treatment of hepatitis C for hemolytic anemia management. *Math Biosci*, 225:141–155, 2010.



- [11] N. M. Dixit, J. E. Layden-Almer, T. J. Layden, and A. S. Perelson. Modelling how ribavirin improves interferon response rates in hepatitis C virus infection. *Nature*, 432:922–924, 2004.
- [12] J. Dushoff, W. Huang, and C. Castillo-Chavez. Backwards bifurcations and catastrophe in simple models of fatal diseases. *J. Math. Biol.*, 36:227–248, 1998.
- [13] Z. Feng, C. Castillo-Chavez, and A. Capurro. A model for tuberculosis with exogenous reinfection. *Theor. Pop. Biol.*, 57:235–247, 2000.
- [14] M. W. Fried, M. L. Shiffman, K. R. Reddy, C. Smith, G. Marinos, F. L. Goncales Jr, D. Hussinger, M. Diago, G. Carosi, D. Dhumeaux, A. Craxi, A. Lin, J. Hoffman, and J. Yu. Peginterferon alfa-2a plus ribavirin for chronic hepatitis C virus infection. *N. Engl J Med*, 347:975–982, 2002.
- [15] M. G. Ghany, D. B. Strader, D. L. Thomas, and L. B. Seeff. Diagnosis, management, and treatment of hepatitis C: An update. *Hepatology*, 49(4):1335–1374, April 2009.
- [16] H. Gomez-Acevedo and M. Y. Li. Backward bifurcation in a model HTLV-I infection of CD<sup>+</sup> T cells. *Bulletin of Mathemation Biology*, 67:101–114, 2005.
- [17] B. Hellriegel. Immunoepidemiology bridging the gap between immunology and epidemiology. *Trends in Parasitology*, 17:102–106, 2001.
- [18] D. M. Jensen, P. Marcellin, B. Freilich, P. Andreone, A. D. Bisceglie, C. E. Brando-Mello, K. R. Reddy, A. Craxi, A. O. Martin, G. Teuber, D. Messinger, J. A. Thommes, and A. Tietz. Re-treatment of patients with chronic hepatitis c who do not respond to peginterferon-  $\alpha$  2b: A randomized trial. *Ann Intern Med*, 150:528–540, 2009.
- [19] D. M. Jensen, T. R. Morgan, P. Marcellin, P. J. Pockros, K. R. Reddy, S. J. Hadziyannis, P. Ferenci, A. M. Ackrill, and B. Willems. Early identification of HCV genotype 1 patients responding to 24 weeks peginterferon alpha-2a (40 kd)/ribavirin therapy. *Hepatology*, 43:954–960, 2006.
- [20] C. M. Kribs-Zaleta and M. Martcheva. Vaccination strategies and backward bifurcation in an age-since-infection structured model. *Math Biosci*, 177 & 178:317–332, 2002.
- [21] N. P. Lam, A. U. Neumann, D. R. Gretch, T. E. Wiley, A. S. Perelson, and T. J. Layden. Dose-dependent acute clearance of hepatitis C genotype 1 virus with interferon alpha. *Hepatology*, 26:226–231, 1997.
- [22] S. S. Lee and P. Ferenci. Optimizing outcomes in patients with hepatitis C virus genotype 1 or 4. *Antiviral Therapy*, 13 Suppl1:9–16, 2008.
- [23] M. Narkowicz, R. Cabrera, and R. Gonzlez-Peralta. The "C" of viral hepatitis in children. *Seminars in Liver Disease*, 27:295–311, 2007.

- [24] U. A. Neumann, N. P. Lam, H. Dahari, D. R. Gretch, T. E. Wiley, T. J. Layden, and A. S. Perelson. Hepatitis C viral dynamics in vivo and the antiviral efficacy of interferon-alpha therapy. *Science*, 282(2):103–107, October 1998.
- [25] R. Qesmi, J. Wub, J. Wua, and J. M. Heffernan. Influence of backward bifurcation in a model of hepatitis B and C viruses. *Math Biosci*, 224:118125, 2010.
- [26] T. C. Reluga, H. Dahari, and A. Perelson. Analysis of hepatitis C virus infection models with hepatocyte homeostasis. *SIAM J. Appl. Math.*, 69(4):999–1023, 2009.
- [27] L. B. Seeff. Natural history of chronic hepatitis C. *Hepatology*, 36:S35–S46, 2002.
- [28] P. M. A. Sloot, A. V. Boukhanovsky, W. Keulen, A. Tirado-Ramos, and C. A. Boucher. A grid-based hiv expert system. *Journal of Clinical Monitoring and Computing*, 19(4-5):263–278, 2005.
- [29] E. Snoeck, P. Chanu, M. Lavielle, P. Jacqmin, E. Jonsson, K. Jorga, T. Goggin, J. Grippo, N. Jumbe, and N. Frey. A comprehensive hepatitis C viral kinetic model explaining cure. *Nature*, 87(706-713):6, June 2010.
- [30] J. Wong, G. McQuillan, J. McHutchison, and T. Poynard. Estimating future hepatitis C morbidity, mortality, and costs in the United States. *Am J Public Health*, 90(10):1562–1569, 2000.
- [31] J. W. Yu, G. Q. Wang, L. J. Sun, X. G. Li, and S. C. Li. Predictive value of rapid virological response and early virological response on sustained virological response in HCV patients treated with pegylated interferon alpha-2a and ribavirin. *J. Gastroenterol Hepatol*, 22:832–836, 2007.